Mon. Not. R. Astron. Soc. **000**, 000–000 (0000) Printed 1 February 2008 (MN LATEX style file v1.4)

The Cluster Substructure - Alignment Connection

Manolis Plionis[1] & Spyros Basilakos[2]
[1] *Institute of Astronomy & Astrophysics, National Observatory of Athens, I.Metaxa & B.Pavlou, Palaia Penteli, Athens 152 36, Greece*
[2] *Astrophysics Group, Imperial College London, Blackett Laboratory, Prince Consort Road, London SW7 2BW, UK*

1 February 2008

ABSTRACT
Using a sample of 903 APM clusters we investigate whether their dynamical status, as evidenced by the presence of significant substructures, is related to the large-scale structure of the Universe. We find that the cluster dynamical activity is strongly correlated with the tendency of clusters to be aligned with their nearest neighbour and in general with the nearby clusters that belong to the same supercluster. Furthermore, dynamically active clusters are more clustered than the overall cluster population. These are strong indications that clusters develop in a hierarchical fashion by anisotropic merging along the large-scale filaments within which they are embedded.

Keywords: galaxies: clusters: general - large-scale structure of universe

1 INTRODUCTION

An interesting observable, that was thought initially to provide strong constraints on theories of galaxy formation, is the tendency of clusters to be aligned with their nearest neighbour as well as with other clusters that reside in the same supercluster (cf. Binggeli 1981; West 1989; Plionis 1994; Chambers, Melott & Miller 2001). Analytical and numerical work have shown that such alignments, expected naturally to occur in "top-down" scenarios (cf. Zeldovich 1970), are also found in hierarchical clustering models of structure formation like the CDM (Bond 1986; West et al. 1991; Splinter et al. 1997; Onuora & Thomas 2000). This fact could be explained as the result of an interesting property of Gaussian random fields that occurs for a wide range of initial conditions and which is the "cross-talk" between density fluctuations on different scales. Furthermore, there is strong evidence that the brightest galaxy (BCGs) in clusters is aligned with the orientation of its parent cluster and even with the orientation of the large-scale filamentary structure within which they are embedded (cf. Struble 1990; West 1994, Fuller, West & Bridges 1999).

Within the framework of hierarchical clustering, the anisotropic merger scenario of West (1994), in which clusters form by accreting material along the filamentary structure within which they are embedded, provides an interesting explanation of such alignments as well as of the observed strong alignment of BCGs with their parent cluster orientation. In this framework, one should expect that dynamical young clusters, at there early stages of formation in which they are not smooth and spherically symmetric, should show substructures that are aligned with the local large-scale structures, an effect observed also in numerical simulations for a variety of power-spectra (van Haarlem & van de Weygaert 1993; Tormen 1997). Indeed, supporting this view West, Jones & Forman (1995) found, using 43 Einstein clusters that have a neighbour within $\sim 10\ h^{-1}$ Mpc, that cluster substructures do show a tendency to be aligned with the orientation of the major axis of their parent cluster and with the nearest-neighbouring cluster (see also Novikov et al 1999). In this work we investigate the relation between the strength of cluster-cluster alignments and the large-scale environment in which the clusters are embedded using the APM cluster catalogue (Dalton et al 1997), which is the largest one available.

2 METHODOLOGY

The APM cluster catalogue is based on the APM galaxy survey which covers an area of 4300 square degrees in the southern sky containing about 2.5 million galaxies brighter than a magnitude limit of $b_J = 20.5$ (for details see Maddox et al. 1990). Dalton et al (1997) applied an object cluster finding algorithm to the APM galaxy data using a search radius of 0.75 h^{-1} Mpc in order to minimize projection effects, and so produced a list of 957 clusters with $z_{est} \lesssim 0.13$. Out of these 309 ($\sim 32\%$) are ACO clusters, while 374 ($\sim 39\%$) have measured redshifts (179 of these are ACO clusters). The APM clusters that are not in the ACO list are relatively poorer systems than the Abell clusters, as we have verified comparing their APM richness's (see Dalton et al 1997 for definition of richness).

For the present analysis we use 903 of the above APM clusters, since 54 clusters are found in the vicinity of plate-holes or crowded regions, a fact which affects severely their shape parameters. The cluster distance is estimated from their redshift using $H_\circ = 100h$ km s^{-1} Mpc^{-1} and $q_\circ = 0.5$.

2.1 Cluster Shape Parameters and Alignment Measure

A detailed analysis of the cluster shape determination procedure and of the intrinsic APM cluster shapes can be

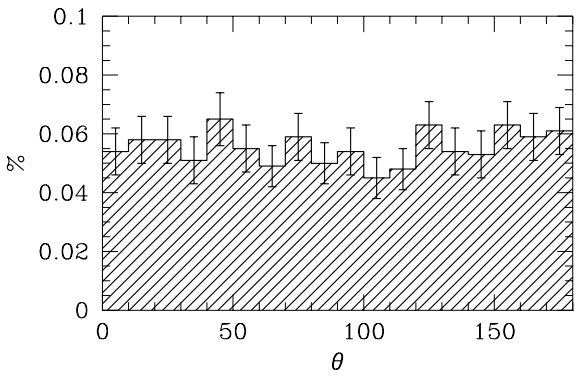

Figure 1. Distribution of APM cluster position angles.

found in Basilakos, Plionis & Maddox (2000). Here we only sketch the basic procedure which is based on the familiar moments of inertia method with $I_{11} = \sum w_i(r_i^2 - x_i^2)$, $I_{22} = \sum w_i(r_i^2 - y_i^2)$, $I_{12} = I_{21} = -\sum w_i x_i y_i$, where x_i and y_i are the Cartesian coordinates of the galaxies that their projected separation is such that they are judged as belonging to the cluster (details in Basilakos et al 2000) and w_i is their weight. We, then diagonalize the inertia tensor solving the basic equation:

$$det(I_{ij} - \lambda^2\, M_2) = 0, \tag{1}$$

where M_2 is the 2×2 unit matrix. The cluster ellipticity is given by $\epsilon = 1 - \frac{\lambda_2}{\lambda_1}$, where λ_i are the positive eigenvalues with $(\lambda_1 > \lambda_2)$. This method can be applied to the data using either the discrete or smoothed distribution of galaxies. The determination of the cluster orientation is consistent among the two methods but this is not true also for the cluster ellipticity (for details see Basilakos et al. 2000)

In Figure 1 we present the derived cluster position angle, θ_i, distribution. We see no significant systematic orientation effects, a fact that we quantify estimating the Fourier transform of the galaxy position angles; $C_n = \sqrt{\frac{2}{N}}\sum \cos 2n\theta_i$ and $S_n = \sqrt{\frac{2}{N}}\sum \sin 2n\theta_i$. If the galaxy position angles are uniformly distributed between 0° and 180°, then both C_n and S_n have zero mean and unit standard deviation. Therefore large values $(> 2.5 - 3)$ indicate significant deviation from isotropy. We find that $C_{1,2}$ and $S_{1,2}$ have values $\lesssim 1.2$, which indicates that there is no systematic orientation bias.

In order to investigate the alignment between cluster orientations, we define the relative position angle between the major axis orientation of a cluster and the direction to a neighbouring one by $\phi_{i,j} \equiv |\theta_i - \vartheta_j|$ (where ϑ is the position angle of the cluster pair separation vector). In an isotropic distribution we will have $\langle\phi_{i,j}\rangle \simeq 45^\circ$. A significant deviation from this would be an indication of an anisotropic distribution which can be quantified by (Struble & Peebles 1995):

$$\delta = \sum_{i=1}^{N} \frac{\phi_{i,j}}{N} - 45 \tag{2}$$

In an isotropic distribution we have $\langle\delta\rangle \simeq 0$, while the standard deviation is given by $\sigma = 90/\sqrt{12N}$. A significantly negative value of δ would indicate alignment and a positive misalignment. To avoid problems related to ill defined position angles we will use in our analysis only clusters that have ellipticities > 0.05 (ie., $N = 888$)*. It should be noted that systematic biases and projection effects will tend to mask any true alignment signal. For example, the projection of foreground galaxies along the line of sight of a cluster as well as the projection on the plane of the sky of member galaxies, always work in the direction of smearing alignments.

2.2 Substructure Measure & Significance

Major obstacles in attempting to determine the dynamical state of a cluster is (1) the ambiguity in identifying cluster substructure in 2D or even 3D cluster data and (2) the uncertainty of post-merging relaxation timescales. Evrard et al. (1993) and Mohr et al. (1995) have suggested as an efficient indicator of cluster substructure the shift of the center-of-mass position as a function of density threshold above which it is estimated. The *centroid-shift* (*sc*) is defined as the distance between the cluster center-of-mass, $(x_{\rm o}, y_{\rm o})$, which may change at different density thresholds and the highest cluster density-peak, $(x_{\rm p}, y_{\rm p})$, ie., $sc = \sqrt{(x_{\rm o} - x_{\rm p})^2 + (x_{\rm o} - x_{\rm p})^2}$.

Kolokotronis et al. (2001), using in a complementary fashion optical and X–ray data (see also Rizza et al. 1998), since in the X-ray band projection effects are minimal, calibrated various substructure measures using APM data and pointed ROSAT observations of 22 Abell clusters and found that in most cases using X–ray or optical data one can identify substructure unambiguously. Only in $\sim 20\%$ of the clusters that they studied did they find projection effects in the optical that altered the X-ray definition of substructure. An important conclusion of Kolokotronis et al. (2001) was that a large and significant value of *sc* is a clear indication of substructure in APM optical cluster data.

The significance of such centroid variations to the presence of background contamination and random density fluctuations are quantified using Monte Carlo cluster simulations in which, by construction, there is no substructure. For each APM cluster, 1000 simulated clusters are produced having the observed ellipticity, the observed number of galaxies, following a King's profile, as well as a random distribution of expected background galaxies, determined by the distance of the cluster and the APM selection function (note that the number of "galaxies" that we allow to follow the King's profile is the observed number minus the expected random background). The King-like profile is:

$$\Sigma(r) \propto \left[1 + \left(\frac{r}{r_{\rm c}}\right)^2\right]^{-\alpha}, \tag{3}$$

where $r_{\rm c}$ is the core radius. We use the weighted, by the sample size, mean of most recent r_c and α determinations (cf. Girardi et al. 1998), i.e., $r_{\rm c} \simeq 0.085\ h^{-1}$ Mpc and $\alpha \simeq 0.7$. We do test the robustness of our results for a plausible range of these parameters (details can be found in Kolokotronis et al. 2001).

Naturally, we expect the simulated clusters to generate small *sc*'s and in any case insignificant shifts. Therefore,

* Our results remain unaltered even for higher values of the ellipticity cutoff.

from each set of Monte-Carlo cluster simulations we derive $\langle sc \rangle_{\rm sim}$ as a function of the same density thresholds as in the real cluster case. Then, within a search radius of 0.75 h^{-1} Mpc from the simulated highest cluster peak, we calculate the quantity:

$$\sigma = \frac{\langle sc \rangle_{\rm o} - \langle sc \rangle_{\rm sim}}{\sigma_{\rm sim}} \ , \qquad (4)$$

which is a measure of the significance of real centroid shifts as compared to the simulated, substructure-free clusters. Note that $\langle sc \rangle_{\rm o}$ is the average, over three density thresholds, centroid shift for the real APM cluster.

A further possible substructure identification procedure is based on a friend-of-friends algorithm, applied on 3 overdensity thresholds of each cluster (for details see Kolokotronis et al. 2001). Three categories are identified, based on the subgroup multiplicity and size: *(a)* No substructure (unimodal), *(b)* Weak substructure (multipole groups but with total group mass $\leq 25\%$ of main), *(c)* Strong substructure (multipole groups but with mass $> 25\%$ of main).

3 RESULTS & DISCUSSION

3.1 Cluster Substructure and Alignments

Applying the *centroid shift* substructure identification procedure to the 903 APM clusters we find that about 30% of clusters have significant ($> 3\sigma$) substructure. Note that defining as having significant substructure those clusters with $\sigma > 2.5$ or 2 increases the fraction to $\sim 40\%$ and 50% respectively. Furthermore, changing the structural parameters of the Monte-Carlo clusters changes the actual σ-values, although their relative significance rank-order remains unaltered. Alternatively if we apply the *subgroup* categorization procedure we find that $\sim$53% of the APM clusters show strong indications of substructure.

We have tested whether there is any systematic redshift dependent effect of the cluster substructure categorization and found none (using either measured or estimated redshifts). We conclude that irrespectively of the method $\sim 30\% - 50\%$ of the APM clusters show indications of significant substructure (in accordance with Kolokotronis et al 2001).

We now test whether the well known nearest-neighbour alignment effect, present in the Abell clusters (cf. Bingelli 1982; Plionis 1994), is evident also in the poorer APM clusters. In table 1 we present, for the whole APM cluster sample, our alignment results as a function of maximum intercluster separation, D_{max}, for both the nearest-neighbours (δ_{nn}) and for all neighbouring pairs (δ_{an}), within D_{max}.

It is evident that there is significant indication of cluster alignments, with the alignment signal dropping in amplitude and significance, as a function of increasing D_{max}. In order to test whether this result is dominated by the ACO cluster pairs, and thus whether it is a manifestation of the already known Abell cluster alignment effect, we have excluded such pairs (113/888 for the *nn*-case) to find consistent but more significant alignment results. For example for the $D_{max} = 15$ h^{-1} Mpc case, we obtain $\langle \delta_{nn} \rangle \simeq -4.3 \pm 1.3$ with $P(> \chi^2) = 0.0004$ and $\langle \delta_{an} \rangle \simeq -2.7 \pm 0.9$ with $P(> \chi^2) = 0.001$.

Note that a large number of APM clusters have estimated redshifts and thus the cluster distance uncertainties will tend to hide true alignments. Therefore, the measured alignment signal should be considered rather as a lower limit to the true one.

D_{max}	$\langle \delta_{nn} \rangle$	$P(> \chi^2)$	N_{pairs}	$\langle \delta_{an} \rangle$	$P(> \chi^2)$	N_{pairs}
5	-7.7±2.7	0.005	90	-7.5 ±2.5	0.002	110
10	-4.6±1.6	0.005	270	-4.1±1.3	0.000	374
15	-3.8±1.2	0.001	444	-2.6±0.9	0.002	848
20	-2.9±1.0	0.004	616	-1.1±0.7	0.023	1602
30	-1.7±0.9	0.069	805	-0.9±0.4	0.112	4012

Table 1. Nearest neighbour (*nn*) and all-neighbour (*an*) alignment signal as a function of maximum pair separation, D_{max}. The χ^2 probabilities are derived by comparing the binned ϕ-distribution (using 3 bins of 30° width) with the Poisson expectation values.

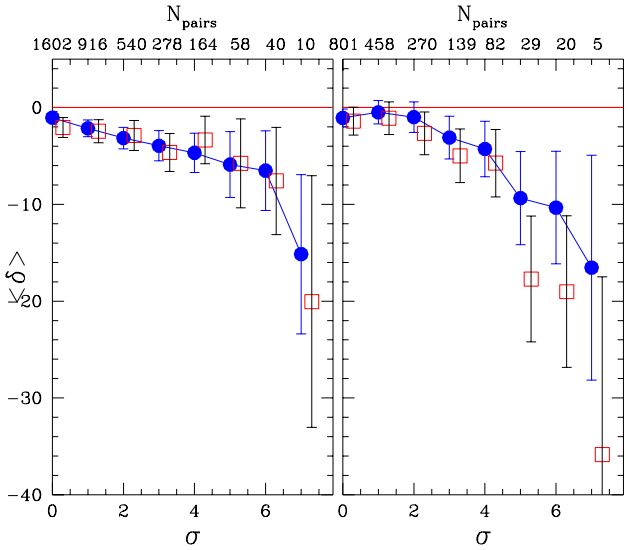

Figure 2. Alignment signal of all cluster pairs with separation $D_{cc} \leq 20$ h^{-1} Mpc, as a function of substructure significance, σ. The left panel presents alignments between cluster major axis orientation and the direction to a neighbour while the right panel represents the alignments between the two cluster major axes orientation. Furthermore, the filled symbols represent the signal based only on the *centroid-shift* substructure categorization while the open symbols represent the signal from clusters that are also categorized as having *strong* substructure by the *subgroup* categorization procedure.

3.2 The Substructure-Alignment Connection

We have correlated the alignment signal with the substructure significance indication in order to see whether there is any relation between the large-scale environment, in which the cluster distribution is embedded, and the internal cluster dynamics.

In figure 2 we present the alignment signal, $\langle \delta \rangle$, between all cluster pairs with separations < 20 h^{-1} Mpc that have substructure significance above the indicated σ value. Evidently, there is a strong correlation between the strength of the alignment signal and the substructure significance level (the two panels are based on slightly different definition of the alignment signal - see caption for details).

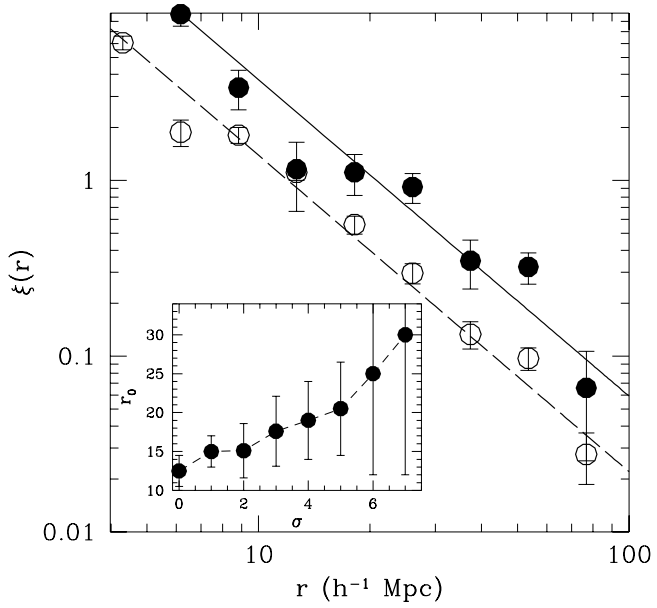

Figure 3. Two-point correlation function of all APM clusters (open symbols) and of $\sigma > 4$ clusters (filled symbols). The lines represent the best $(r/r_\circ)^{-1.8}$ fit with $r_\circ \simeq 12$ and $\simeq 20\ h^{-1}$ Mpc respectively. Insert: The cluster correlation length as a function of substructure significance.

In order to assess the statistical significance of obtaining such a $\delta - \sigma$ relation, we perform a large number (10000) of Monte-Carlo simulations in which we reshuffle the measured position angles, assigning them at random to the clusters. Then we derive the corresponding $\delta - \sigma$ relation and count in how many such simulations do we get values of δ which are as negative, or more, than the corresponding ones of figure 2. We find that the corresponding probability is $< 10^{-5}$, while for the less restrictive case, of having negative δ-values (of any amplitude) for all σ, the probability is again quite small ($\sim 7.5 \times 10^{-3}$).

Note that from the analysis of Kolokotronis et al (2001) it is expected that our procedure will misidentify the dynamical state of $\sim 20\%$ of the APM clusters. However, such misidentification will act as a noise factor and will tend to smear any true alignment-substructure correlation, since there is no physical reason why random projection effects, within 0.75 h^{-1} Mpc of the cluster core, should be correlated with the direction of neighbours within distances up to a few tens of Mpc's (such a correlation could be expected at some level only for nearest-neighbours in angular space but we have verified that choosing such pairs we obtain an insignificant alignment signal). Therefore our result, based on the largest cluster sample available, supports the hierarchical clustering scenario and in particular the formation of cluster by anisotropic merging along the filamentary structure within which they are embedded (cf. West 1994; West, Jones & Forman 1995).

3.3 Local density - Substructure Correlation

If the above view is correct then one would expect that clusters with significant substructure should be residing preferentially in high-density environments (superclusters), and this would then have an imprint in their spatial two-point correlation function.

In figure 3 we present the spatial 2-point correlation function of all APM clusters (open symbols) and of those with substructure significance $\sigma \geq 4$ (filled symbols). It is clear that the latter are significantly more clustered. This can be seen also in the insert of figure 3 were we plot the correlation length, r_0, as a function of σ, which is clearly an increasing function of cluster substructure significance level. Note that in order to take into account the possible systematic distance dependent effects in the different cluster subsamples we generate random catalogues, used to normalize the number of cluster-cluster pairs in the $\xi(r)$ estimate, using the individual distance distribution of each subsample and not the overall APM cluster selection function. Had we used the latter, the increase of $r_\circ$ with σ would have been more severe.

Furthermore, we have tested whether this effect could be due to the well-known richness dependence of the correlation strength, and found a weak, if any, such richness trend. In order to further investigate this issue we have correlated the APM richness (see Dalton et al 1997) with σ and found a very weak but significant correlation (the Pearson's coefficient is only 0.26 but with a significance >99.9%). Therefore, a component contributing to the increase of the $r_\circ(\sigma)$ function could possibly be the cluster richness effect (through the above richness-σ weak correlation). However, the increase of $r_\circ(\sigma)$ is quite dramatic and cannot be attributed only to this weak richness dependence. This is corroborated also from the fact that there is a larger fraction of clusters with significant substructure (high σ values) residing in high-density regions (superclusters), as shown in figure 4 where we plot the fraction of clusters with $\sigma > 3$ that belong to superclusters identified by the indicated percolation radius. Evidently the fraction increases inversely with percolation radius. These results are similar to those of Schombert & West (1990) based on Abell clusters, in which they found that flattened clusters, flatness being an indication of dynamical youth, are more frequent in high density environments (see however Herrera & Sanroma 1997 for a different view).

The conclusion of this correlation function analysis is that indeed the clusters showing evidence of dynamical activity reside in high-density environments, as anticipated from the alignment analysis. It is interesting that such environmental dependence has also been found in a similar study of the BCS and REFLEX clusters (Schüecker et al. 2001) and for the cooling flow clusters with high mass accretion rates (Loken, Melott & Miller 1999).

4 CONCLUSIONS

We have presented evidence, based on the largest available cluster sample, the APM, that there is a strong link between the dynamical state of clusters and their large-scale environment. Clusters showing evidence of dynamical activity are significantly more aligned with their nearest neighbours and they are also much more spatially clustered. This supports the hierarchical clustering models in which clusters develop

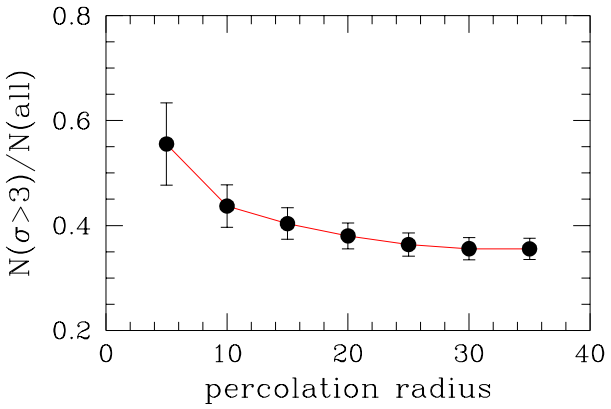

Figure 4. The fraction of clusters with significant substructure ($\sigma > 3$) that reside in superclusters, defined by the indicated percolation radius.

by accreting matter along the large-scale filamentary structures within which they are embedded.

ACKNOWLEDGEMENTS

M.Plionis acknowledges the hospitality of the Astrophysics Group of Imperial College. This work was partially supported by the EC Network programme 'POE' (grant number HPRN-CT-2000-00138). We thank the referee, M.West, for very helpful suggestions that improved our work.

REFERENCES

Basilakos S., Plionis M., Maddox S. J., 2000, MNRAS, 315, 779
Bingelli B., 1982, AA, 250, 432
Bond, J.R., 1986, in *Galaxy Distances and Deviations from the Hubble Flow*, eds. Madore, B.F., Tully, R.B., (Dordrecht: Reidel), p.255
Chambers, S.W., Melott, A.L., Miller, C.J., 2001, ApJ, in press, *(astro-ph/0102218)*
Dalton G. B., Maddox S. J., Sutherland W. J., Efstathiou G., 1997, MNRAS, 289, 263
Evrard A.E., Mohr J.J., Fabricant D.G., Geller M.J.,1993, ApJ, 419, L9
Fuller, T.M., West, M.J. & Bridges, T.J., 1999, ApJ, 519, 22
Girardi M., Giuricin G., Mardirossian F., Mezzetti M., Boschin W., 1998, ApJ, 505, 74
van Haarlem, M., van de Weygaert, R., 1993, ApJ, 418, 544
Herrera, B., Sanroma, M., 1997, AA, 320, 13
Kolokotronis, V., Basilakos, S., Plionis, M., Georgantopoulos, I., 2001, MNRAS, 320, 49
Loken, C., Melott, A.L., Miller, C.J., 1999, ApJ, 520, L5
Maddox S.J. , Sutherland W.J., Efstathiou G., Loveday, J. 1990, MNRAS, 243, 692
Mohr, J.J., Evrard, A.E., Fabricant, D.G., Geller, M.J., 1995, ApJ, 447, 8
Novikov, D. et al., 1999, MNRAS, 304, L5
Onuora, L.I., Thomas, P.A, 2000, MNRAS, 319, 614
Plionis M., 1994, ApJS., 95, 401
Plionis M., 2001, in the proceedings of the *Clusters and the High-Redshift Universe observed in X-rays*, XXI$^{\rm th}$ Moriond Astrophysics Meeting, eds. Neumann et al., *in press*
Richstone, D., Loeb, A., Turner, E.L., 1992, ApJ, 393, 477
Rizza E., Burns J. O., Ledlow M. J., Owen F. N., Voges, W., Blito M., 1998, MNRAS, 301, 328
Schombert, J. M., West, M. J., 1990, ApJ, 363, 331
Schüecker, P., Böhringer, H., Reiprich, T. H., Feretti, L., AA, 2001, 378, 408
Splinter, R.J., Melott, A.L., Linn, A.M., Buck, C., Tinker, J., 1997, ApJ, 479, 632
Struble, M.F., 1990, AJ, 99, 743
Struble, M.F., Peebles, P.J.E., 1985, AJ, 90, 582
Tormen, G., 1997, MNRAS, 290, 411
West, M. J., 1989, ApJ, 347, 610
West, M. J., Villumsen, J.V., Dekel, A., 1991, ApJ, 369, 287
West, M. J., 1994, MNRAS, 268, 79
West, M. J., Jones C., Forman W., 1995, ApJ, 451, L5
Zeldovich, Y.B., 1970, AA, 5, 84